Data-Driven Fault Classification of Induction Motor Based on Recurrence Plot and Deep Convolution Neural Network

Rafia Nishat TOMA, Yangde GAO and Jong-Myon KIM[1]
Department of Electrical, Electronics and Computer Engineering,
University of Ulsan, Ulsan, Korea

Abstract. Condition monitoring becomes an integral part of the industrial manufacturing system to ensure a safe working environment and reduce the cost of maintenance. Involving deep learning techniques in fault diagnosis methods not only increases the accuracy and reliability of the system but also reduces the operation time and hassle of the manual feature extraction process. In this paper, a complete framework for fault classification is introduced by using the vibration signals of bearings containing normal and faulty conditions. Firstly, the frequency spectrums of the time-series signals are generated with FFT and transformed the 1-D signal into 2-D images with the recurrence plots (RP) algorithm. Finally, a deep CNN model is designed to classify the bearing conditions with the extracted high-level features from the RP-based image dataset. The images show a distinct pattern in every bearing condition and the CNN model can achieve 99.24% accuracy to classify three different bearing conditions. The image classification-based fault diagnosis approach is automated and eliminates the disadvantages of the manual feature extraction process. The generated images with RP were also trained with three predefined CNN models to verify the effectiveness of the fault patterns. Finally, the comparative analysis demonstrates that the proposed method outperforms other researchers' approaches both in terms of classification accuracy and computational cost.

Keywords. Bearing fault classification, convolutional neural networks (CNN), frequency spectrum, image representation of vibration signal, recurrence plot (RP)

1. Introduction

The vibration signals are the most used signal type in the fault diagnosis approaches of induction motors (IM) due to the convenient installation process of vibration sensors and the integrity of the collected data [1]. Some benefits of IMs, such as simple design, low-cost and high fabricating technologies, and reliable operating ability make them an inseparable component in modern industries. Sudden failure of any components due to long operating time, tough working environment, and varying load can result in both economic and health hazards on a large scale. To ensure the continuous operation and high reliability of the system, the importance of performing predictive maintenance cannot be ignored [2]. The IEEE survey found that the bearing fault was the most

---

[1] Corresponding Author: Jong-Myon Kim, Department of Electrical, Electronics and Computer Engineering, University of Ulsan, Ulsan, Korea; E-mail: jmkim07@ulsan.ac.kr.

occurring and covered more than 40% of the total mechanical failures [3]. The fault diagnosis of the rolling element bearings can be classified mainly as a model-based and data-driven method. A mathematical model is designed with the assumptions of the real system and compares the result with the corresponding data of the system to predict the health conditions of the bearings [4]. The data-driven technique mainly extracts features from the data of different bearing health conditions and classifies them with machine learning (ML) models. Different types of signals from induction motors such as vibration signal, current signal, acoustic emission signal, and temperature are acquired and investigated to analyze faulty conditions in condition monitoring. Multiple features from the time domain, frequency domain, and time-frequency domain are extracted from the acquired signal, but due to the non-linear and non-stationary nature of bearing data, all extracted features may not equally exhibit fault signatures and a feature selection technique is required. However, the successful implementation of this overall process needs a good knowledge of the acquired data and expertise in the signal processing techniques [5]. Advanced ML methods, such as deep learning (DL) techniques, named autoencoder (AE), deep belief networks (DBN), artificial neural network (ANN), and convolutional neural network (CNN) can successfully overcome the limitations of manual ML algorithms by automatically extracting significant features from the original data [6].

Despite CNNs' ability to learn patterns directly from raw data, the raw data are often heavily contaminated by noise from the outside environment. Therefore, CNNs have been combined with different domain-based processing algorithms to improve fault-diagnosis systems. The generation of images from 1-D signals by using wavelet packet transforms (WPT), spectrograms, and Gramian angular field (GAF), and classifying them with a 2-D CNN model has become very efficient in fault diagnosis fields [5]. A detailed discussion on fault diagnosis of IM can be found in [7].

2. Experimental setup

The vibration signal used in this study is taken from the KAT-bearing dataset by the Kat-Data Center of Paderborn University [8]. The overall experimental test rig of the dataset is shown in Figure 1.
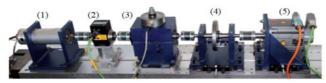

Figure 1. An experimental testbed of collecting bearing data.

Here, a 425-W Hanning synchronous motor (Type SD4CDu8S-009) was used as the test drive motor, and an inverter (KEB Combivert 07F5E 1D-2B0A) with a 16 kHz switching frequency was employed to control its operation. This dataset contains different types of signals from five sensors, which include vibration signal, current signal with two different phases, load torque, and radial forces on the bearings. The vibration signal was recorded by a piezoelectric accelerometer with a sampling rate of 64 kHz for several working conditions, where different values of the rotational speed, radial force, and load torque were considered. In this study, we considered 17 bearings signals and divided them into three different health conditions, named normal (N), outer race fault

(OF), and inner race fault (IF). The initiated "damage/fault" had been prepared according to ISO 15243. The bearing code of the respective bearing conditions with the label is listed in Table 1.

Table 1. Bearing code with the health condition.

Type	Bearing Code	Label
Normal (N)	K001, K002, K003, K004, K005, K006	0
Outer race fault (OF)	KA04, KA15, KA16, KA22, KA30	1
Inner race fault (IF)	KI04, KI14, KI16, KI17, KI18, KI21	2

3. Materials and methods

Rolling element bearings may sustain a variety of types of mechanical damages throughout their long-term use in industrial environments because of incorrect installation, manufacturing error, and material fatigue. We considered two different faulty conditions of bearings, named outer race fault and outer race fault. The respective fault frequency can be expressed with the Eqs. (1) and (2) as given below [9]:

Outer race fault freq.:
$$f_o = \frac{N_{ball}}{2}.f_m.\left(1 - \frac{D_{ball}}{D_{cage}}.cos\beta\right) \tag{1}$$

Inner race Fault freq.:
$$f_i = \frac{N_{ball}}{2}.f_m.\left(1 + \frac{D_{ball}}{D_{cage}}.cos\beta\right) \tag{2}$$

Where N_{ball} defines the number of rolling elements, D_{ball} and D_{cage} represent the rolling element and cage diameter, respectively. β indicates the angles of the load from the radial plane and f_m denotes the rotational frequency of bearing.
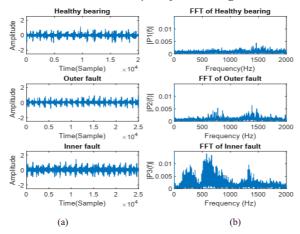

(a)   (b)

Figure 2. (a) Time and (b) Frequency spectrums of the vibration signal for three different health conditions.

An imaging method based on vibration signal is proposed to classify different types of bearing faults in IM with CNN in this work. The overall method can be divided into two parts. The first part converts the 1-D time-series vibration signal into 2-D images and in the second part, a customized CNN model is designed to classify the images in

respective bearing conditions. As discussed earlier, there exist different fault frequencies depending on the type of occurring fault in the bearings, we generate the frequency spectrum from the time domain signal for all the considering bearing conditions (Figure 2(b)) and found that frequency-domain signals were more suitable to generate distinct patterns among the bearing condition with RP.

The FFT outputs of the time-series signals show that each bearing condition reveals a different frequency spectrum due to the different fault types and characteristics frequency of the bearings. The recurrence analysis is considered one of the promising methods to analyze the nonlinear and non-stationary as well as noisy time-series data obtained from the different experimental testbeds. The term "recurrence" can be specified as the occurrence of a specific repetitive state of a dynamic oscillator [10]. Eckmann et al. [11]launched the recurrence plots (RP) method to visualize the trajectory of dynamic systems. The method allows the identification of hidden recurring patterns, non-stationarity, and changes in the system structure.

The recurrence plot can be obtained by following three steps [12]:

Step 1: For an N-length time-series signal $\{x(1), x(2), \ldots, x(N)\}$, the signal will be reconstructed to the 2-D phase space having dimension *m* and delay time τ as Eq (3):

$$X(i) = \{x(i), x(i + \tau), \ldots, x(i + (m - 1))\tau\} \tag{3}$$

Here, $i = 1, 2, \ldots M$, and $M = \{N - (m - 1)\tau\}$, and *M* implies the vector number in the rebuilt phase space.

Step 2: After that, based on the distance between the *i-th* and *j-th* phase point of the reconstructed phase space signal, the recurrence matrix will be generated by Eq (4):

$$R_{i,j} = H(\varepsilon - \|X(i) - X(j)\|), \ i,j = 1, \ldots, N$$
$$= \begin{cases} 1; \varepsilon > \|X(i) - X(j)\|; \\ 0; \varepsilon < \|X(i) - X(j)\|; \end{cases} \tag{4}$$

Here, ε represents the threshold, and H represents the Heaviside function.

Step 3: Finally, with the $R_{i,j}$ values of each horizontal *(i)* and vertical *(j)* coordinate, the recurrence plot will be generated with the matrix. As it always follows, $R_{i,j} = R_{j,i}$, the pattern of the resultant recurrence plot is always symmetric. As a result of texture information, individual dots, sloping lines, perpendicular lines, and horizontal lines can be identified, whereas typology information can be categorized as uniform, shift, regular, and interrupted. The resultant recurrence plots of the frequency spectrum signal of three different bearing conditions are provided in Figure 3.
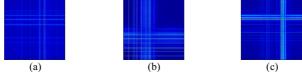

(a)   (b)   (c)

Figure 3. Recurrence Plot of the frequency spectrum signal for (a) Normal, (b) Outer fault , and (c) Inner fault conditions.

Finally, a three-layer deep CNN model is designed to classify the generated RP images and evaluate the model performance with some evaluation matrix. Each stage consists of convolution, activation, and pooling layers and acts as a feature learning stage including different feature levels. A fully connected layer is attached to the convolution layers and the output node of the dense layer is equivalent to the number of considered health conditions, which is three for this study (Healthy bearing, inner race fault, and

outer race fault). The ReLU activation function was applied for all the layers. As part of the CNN training process, two learnable parameters named the network's weight matrix and bias are updated using stochastic gradient descent (SGD). The CNN model requires less pre-processing to efficiently read images with the filters, which makes CNN more efficient in image classification than conventional ML algorithms. As a part of the study, we investigated various configurations and tuning parameters to determine their effect on classification performance, and finally, the most optimum CNN model we found is described in Table 2.

Table 2. The applied CNN architecture

Layer (type)	Output Shape	Learnable Parameters
Input layer	(128×128×3)	0
Convolution layer_1	(128×128×16)	448
BatchNormalization_1	(128×128×16)	32
relu_1	(128×128×16)	0
Max pooling_1	(64×64×16)	0
Convolution layer_2	(64×64×32)	4640
BatchNormalization _2	(64×64×32)	64
relu_2	(64×64×32)	0
Max pooling_2	(32×33×32)	0
Convolution layer_3	(32×33×64)	18496
BatchNormalization _3	(32×33×64)	128
relu_3	(32×33×64)	0
Max pooling _3	(32×31×64)	0
Fully connected (fc)	(1×1×3)	190467
Softmax	(1×1×3)	0
Output layer	-	0

The workflow of the summarized operations of our proposed fault classification methodology is presented in Figure 4.

Figure 4. Proposed methodology of fault classification.

4. Results and discussions

In the experiment, the total number of samples was 1320, where the bearings with the normal condition and the inner race fault contain 460 samples each, and the remaining 400 samples belong to the outer race fault. Among them, 70% (924 images) and 10% (132 images) samples were separated for training and validating the CNN model, respectfully and the remaining 20% (264 images) samples were for testing purposes. To learn the multi-level features from three bearing conditions RP, the CNN model was trained up to 50 epochs. Throughout the training phase, the designed deep CNN model can efficiently learn to generalize features from RP images and can achieve almost 100% accuracy both in training and validation. Finally, the performance of the trained CNN model was measured by the 264 testing samples, and the results were present in the classification report and confusion matrix. To validate the use of frequency spectrum instead of time-domain signal, we generate RP-based images from both time and frequency domain signals and check the classification performance with the same CNN

model. The classification report of the designed model on the test dataset is given in Table 3, which clearly shows that the CNN model extract and learn the features well and finally, classify the features into individual class with the test samples with 99.24% accuracy.

Table 3. Classification Report.

Class	Precision	Recall	F1-Score
Normal	0.99	0.99	0.99
Inner Fault	1.00	1.00	1.00
Outer Fault	0.99	0.99	0.99
Accuracy (%)		99.24	

From the confusion matrix of Figure 5, it shows that the images generate from the original signal have an accuracy of 71.21%, whereas the RPs from the frequency spectrum can classify bearing conditions with more than 99% accuracy with a very low number of misclassification samples.
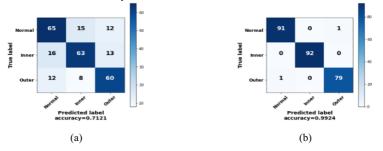

(a)   (b)

Figure 5. Confusion matrix of the CNN model with recurrence plot on (a) Original signal, and (b) frequency spectrum signal.

In addition, three other most commonly used pre-defined CNN models for image classification [13], named GoogleNet (22-layers), ResNet-18 (18-layers), and AlexNet (8-layers) were implemented to train and classify the RP-based images of the bearings to validate the efficiency of the generating image dataset. Figure 6 (a) represents the classification accuracy values for all four CNN models. Along with our designed CNN model, the ResNet-18 and AlexNet can successfully classify RP images with more than 99% accuracy, whereas GoogleNet shows 93.18% accuracy on the test dataset. But the computational complexity is not the same for every model, as it depends on the number of layers of the respective models. We show the model execution time for 50 epochs in Figure 6 (b), which clearly shows that because of having a higher number of layers, all the 3 pre-defined CNN models require a large computational time than our designed CNN model.
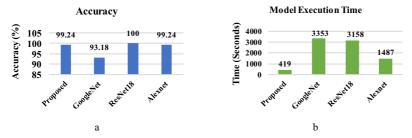

a   b

Figure 6. Comparison of (a) accuracy, and (b) computational complexity of the proposed and three pre-defined CNN models.

In the end, some prior methods have been considered to compare the classification performance of the proposed method applied to the same KAT vibration data. In different studies, the time-series data pattern was changed into the 2-D format, such as 2-D reshaped matrix, grayscale images (vibration/CWT), or RGB images. In addition, various types of pretrained CNN models (TICNN, LeNet-5, VGG16, ResNet)) were also applied to classify the 2-D image samples. The evaluation performances of different approaches are listed in Table 4 based on accuracy and f1-score.

The performance of the CNN models becomes higher with the image input rather than 1-D data in terms of accuracy and f1-score. In addition, the CNN models based on the pre-defined model, such as VGG16 and ResNet have a higher computational cost than the other CNNs. Therefore, from the results provided in Table 4, the proposed signal-to-image conversion-based fault classification approach based on the RP and deep CNN methods show superior performance in terms of accuracy and computational cost.

Table 4. Performance comparison of different methods.

Reference	Applied Method	Accuracy	f1-score	Computational Cost
[14]	Original+TICNN	96.03	96.03	O (90772)
[15]	1-D matrix+CNN	94.49	95.04	O (2117120)
[16]	CWT+VGG16	97.99	97.99	O (138357544)
[17]	RGB+ResNet	99.53	99.53	O (25636712)
[18]	MSF+RGB+CNN	99.99	99.99	O (37467)
This paper	FFT+ RP+CNN	99.24	99.24	O (190467)

5. Conclusions

A comprehensive fault classification approach of bearing is presented based on the recurrence plot-based visualization of time-series signal and deep CNN model. Based on the property of locating the characteristics of fault frequencies from the time-domain signal of FFT, a method of displaying vibration signal frequency spectrums was explored. The raw vibration data acquired from the industrial testbed is often surrounded by noise and very difficult to extract fault information in case of condition monitoring. Different pre-processing mechanisms need to be applied for extracting fault signatures, which requires high expertise in this field. In our study, the 1-D signal observe sequentially and converted images by RP algorithm helps to preserve the temporal features, which resolves the necessity of additional signal processing requirements. The images generate through RP help the deep CNN model to achieve the classification accuracy of 99.24%. In addition, due to image property, it can accomplish the classification task with the CNN model quicker than the other conventional approaches. The overall method does not require much expertise or prior knowledge of extracting features and that makes it more efficient than the manual feature extraction-based process of the traditional ML classification algorithms. Finally, a comparative study was presented with some different 2-D imaging and neural network-based techniques, which proves that the proposed fault classification approach can be an excellent solution in bearing fault diagnosis with great reliability, high accuracy, and low computational cost. Our next phase of research aims to improve the proposed method's ability to handle information from sensors with different sampling frequencies and design an optimized CNN with hyperparameter tuning to make the system more automated.

Acknowledgement

References

[1] Toma RN, Toma FH, Kim JM. Comparative analysis of continuous wavelet transforms on vibration signal in bearing fault diagnosis of induction motor. Proc Int Conf Electron Commun Inf Technol ICECIT 2021. 2021.

[2] Yan X, Liu Y, Jia M, Zhu Y. A multi-stage hybrid fault diagnosis approach for rolling element bearing under various working conditions. IEEE Access. 2019;7:138426–41.

[3] Sihag N, Sangwan KS. A systematic literature review on machine tool energy consumption. J Clean Prod. 2020;275.

[4] Piltan F, Kim JM. Bearing anomaly recognition using an intelligent digital twin integrated with machine learning. Appl Sci. 2021;11(10):4602.

[5] Toma RN, Piltan F, Im K, Shon D, Yoon TH, Yoo DS et al. A bearing fault classification framework based on image encoding techniques and a convolutional neural network under different operating conditions. Sensors [Internet]. 2022 Jun 28;22(13):4881. Available: https://www.mdpi.com/1424-8220/22/13/4881

[6] Fan G, Li J, Hao H. Vibration signal denoising for structural health monitoring by residual convolutional neural networks. Meas J Int Meas Confed. 2020;157.

[7] Liang X, Ali MZ, Zhang H. Induction motors fault diagnosis using finite element method: A review. IEEE Trans Ind Appl. 2020;56(2):1205–17.

[8] Lessmeier C, Kimotho JK, Zimmer D, Sextro W. Condition monitoring of bearing damage in electromechanical drive systems by using motor current signals of electric motors: a benchmark data set for data-driven classification. Third Eur Conf Progn Heal Manag Soc 2016. 2016;(Cm):152–6.

[9] Toma RN, Prosvirin AE, Kim JM. Bearing fault diagnosis of induction motors using a genetic algorithm and machine learning classifiers. Sensors (Switzerland). 2020;20(7).

[10] Ambrożkiewicz B, Syta A, Meier N, Litak G, Georgiadis A. Radial internal clearance analysis in ball bearings. Eksploat i Niezawodn. 2021;23(1):42–54.

[11] Eckmann JP, Oliffson Kamphorst O, Ruelle D. Recurrence plots of dynamical systems. Epl. 1987;4(9):973–7.

[12] Wang F, Zhou D, Zhang S. Mechanical condition monitoring of on-load tap changer based on textural features of recurrence plots of vibration signals. Proc 2019 5th Int Conf Electr Power Equip - Switch Technol Front Switch Technol a Futur Sustain Power Syst ICEPE-ST 2019. 2019;560–4.

[13] Jiao J, Zhao M, Lin J, Liang K. A comprehensive review on convolutional neural network in machine fault diagnosis. Neurocomputing. 2020;417:36–63.

[14] Zhang W, Li C, Peng G, Chen Y, Zhang Z. A deep convolutional neural network with new training methods for bearing fault diagnosis under noisy environment and different working load. Mech Syst Signal Process. 2018;100:439–53.

[15] Xia M, Li T, Xu L, Liu L, De Silva CW. Fault diagnosis for rotating machinery using multiple sensors and convolutional neural networks. IEEE/ASME Trans Mechatronics. 2018;23(1):101–10.

[16] Shao S, McAleer S, Yan R, Baldi P. Highly accurate machine fault diagnosis using deep transfer learning. IEEE Trans Ind Informatics. 2019;15(4):2446–55.

[17] Wen L, Li X, Gao L. A transfer convolutional neural network for fault diagnosis based on ResNet-50. Neural Comput Appl. 2020;32(10):6111–24.

[18] Xie T, Huang X, Choi SK. Intelligent mechanical fault diagnosis using multisensor fusion and convolution neural network. IEEE Trans Ind Informatics. 2022;18(5):3213–23.